Multiple-magnon excitations shape the spin spectrum of cuprate parent compounds

Davide Betto,[1,*] Roberto Fumagalli,[2] Leonardo Martinelli ,[2] Matteo Rossi ,[2] Riccardo Piombo ,[3] Kazuyoshi Yoshimi ,[4]
Daniele Di Castro,[5,6] Emiliano Di Gennaro,[7,8] Alessia Sambri,[8] Doug Bonn,[9] George A. Sawatzky,[9] Lucio Braicovich,[1]
Nicholas B. Brookes,[1] José Lorenzana ,[3,†] and Giacomo Ghiringhelli [2,10,‡]

[1]*European Synchrotron Radiation Facility, B.P. 220, 38043 Grenoble, France*
[2]*Dipartimento di Fisica, Politecnico di Milano, Piazza Leonardo da Vinci 32, 20133 Milano, Italy*
[3]*ISC-CNR and Dipartimento di Fisica, Università di Roma "La Sapienza", Piazzale Aldo Moro 5, 00185 Roma, Italy*
[4]*The Institute for Solid State Physics, The University of Tokyo, Kashiwa-shi, Chiba 277-8581, Japan*
[5]*Dipartimento di Ingegneria Civile e Ingegneria Informatica, Università di Roma Tor Vergata, Via del Politecnico 1, 00133 Roma, Italy*
[6]*CNR-SPIN, Università di Roma Tor Vergata, Via del Politecnico 1, 00133 Roma, Italy*
[7]*Dipartimento di Fisica "E. Pancini", Università degli Studi di Napoli "Federico II", Complesso Monte Sant'Angelo via Cinthia,
80126 Napoli, Italy*
[8]*CNR-SPIN, Complesso Monte Sant'Angelo via Cinthia, 80126 Napoli, Italy*
[9]*Department of Physics and Astronomy, University of British Columbia, Vancouver, British Columbia V6T 1Z1, Canada*
[10]*CNR-SPIN, Dipartimento di Fisica, Politecnico di Milano, Piazza Leonardo da Vinci 32, 20133 Milano, Italy*

Thanks to high resolution and polarization analysis, resonant inelastic x-ray scattering (RIXS) magnetic spectra of La_2CuO_4, $Sr_2CuO_2Cl_2$ and $CaCuO_2$ reveal a rich set of properties of the spin-$1/2$ antiferromagnetic square lattice of cuprates. The leading single-magnon peak energy dispersion is in excellent agreement with the corresponding inelastic neutron scattering measurements. However, the RIXS data unveil an asymmetric line shape possibly due to odd higher order terms. Moreover, a sharp bimagnon feature emerges from the continuum at $(1/2, 0)$, coincident in energy with the bimagnon peak detected in optical spectroscopy. These findings show that the inherently complex spin spectra of cuprates, an exquisite manifestation of quantum magnetism, can be effectively explored by exploiting the richness of RIXS cross sections.

The spin-$1/2$ antiferromagnetic two-dimensional (2D) square lattice is one of the best studied quantum systems and represents a benchmark for quantum magnetism. Notably, it depicts the spin ground state arrangement in the CuO_2 planes, common to all high-temperature superconducting layered cuprates, when no doping charge is present and the antiferromagnetic order impedes charge transport and energetic magnons dominate the spin spectra [1,2]. Upon doping, long range antiferromagnetism is substituted by superconductivity but short range in-plane spin correlations survive, giving rise to damped magnons of comparably high energy [3–6]. Indeed, spin fluctuations are considered to be a main ingredient of the Cooper pairing "glue" in these materials [7], as suggested by the correlation between T_c and the exchange interaction J in certain cuprate families [8–12]. The spectrum of magnetic excitations has been extensively used to experimentally determine the coupling parameters with physical importance [1,2,10,13–20], such as J, the hopping integral t, and the Coulomb repulsion U.

The magnon dispersion is traditionally measured by inelastic neutron scattering (INS) and reproduced, within the linear spin-wave theory, by an improved Heisenberg model that includes higher order terms [2,10,21]. In the last decade resonant inelastic x-ray scattering (RIXS) [22] has proved to be a valid alternative to INS, in particular for cuprates [3,5,6,23,24] and other transition metal compounds with large superexchange coupling [25–29].

Neutrons interact only with the electrons' spin, not with the charge, and with the atomic nuclei, making the theoretical treatment of the scattering cross sections rather straightforward [30]. Consequently, once the phononic background is duly subtracted, the interpretation of the INS experimental spectra in terms of magnetic scattering function is in principle simple but, at the same time, it misses part of the richness of the many-body problem. Instead RIXS allows for a wide energy loss range measured at constant resolving power. Compared with INS it can profit from much larger cross sections and incident flux but requires a more involved theoretical analysis [31,32], with less stringent selection rules. Therefore, RIXS has the potential to provide more information on the problem if one is able to disentangle the complexity of the spectra by exploiting good energy resolution and the analysis of the scattered x-rays' polarization (polarimetric analysis) [33,34].

These differences in the cross sections stimulated a close comparison of the two techniques, and some doubts were raised on the possibility of deriving the actual spin dynamical

*davide.betto@esrf.fr
†jose.lorenzana@cnr.it
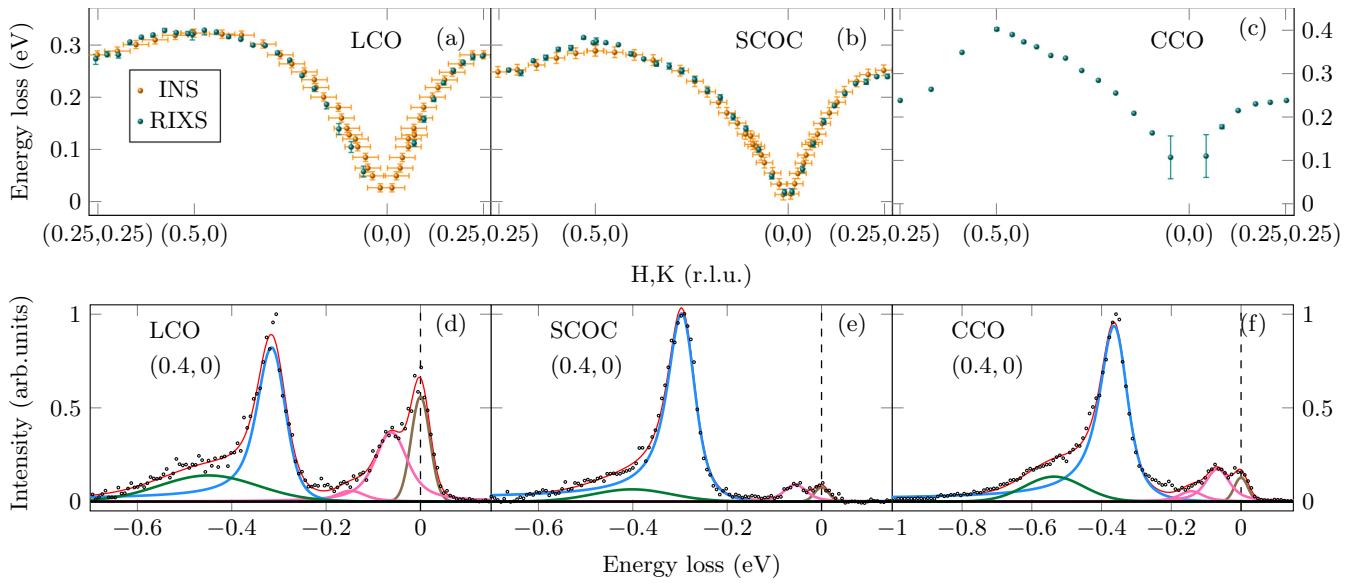‡giacomo.ghiringhelli@polimi.it

FIG. 1. (a)–(c) Single magnon dispersion determined by RIXS for the three compounds and by INS for SCOC and LCO (Refs. [2] and [21], respectively). (d)–(f) RIXS spectra at (0.4,0) measured with π incident photon polarization (black circles) and their main constituents obtained by a phenomenological fitting (red line): Gaussian elastic peak (brown), two resolution limited phonon contributions (pink), single magnon with Fano line shape (blue), even order multimagnons (green).

structure factor $S(\mathbf{q}, \omega)$ from RIXS data. Indeed, in the very first RIXS work Braicovich *et al.* [35] had already shown that in La$_2$CuO$_4$ the single-magnon energy dispersion in INS and RIXS coincide almost perfectly, a fact that has been recently confirmed more extensively [36]. However, Plumb *et al.* [21] pointed out some discrepancies in the magnetic excitation spectrum of Sr$_2$CuO$_2$Cl$_2$ close to $\mathbf{q} = (\frac{1}{2}, 0)$ (X point) of the two-dimensional (2D) Brillouin zone [37], where the RIXS-derived magnon energy exceeds that of INS by $\sim$25 meV, i.e., about 10%. In this Letter, we start from this single-magnon issue and unveil a richer scenario for the RIXS data. We report high-resolution RIXS measurements on a La$_2$CuO$_4$ (LCO) thin film ($\sim$100 nm thick), Sr$_2$CuO$_2$Cl$_2$ (SCOC) crystals, and a CaCuO$_2$ (CCO) thin film, with special emphasis on the low-energy (magnetic) portion of the spectra and on the comparison with the most recent INS data on the same compounds, where available. A polarimetric analysis at selected momentum points, supplemented with theoretical computations, allows us to constrain the symmetry of the different contributions to the RIXS line shape.

The RIXS spectra were acquired using the ERIXS spectrometer of the ID32 beamline [38] at the European Synchrotron ESRF, which includes the polarimeter used for the analysis of the polarization of the scattered light [33,34]. The x-ray energy was tuned to the Cu L_3 edge, at about 931 eV. The incoming x rays were polarized either parallel (π) or perpendicular (σ) to the scattering plane (see Supplemental Material (SM) Fig. S1 [39]). The total energy resolution was $\sim$47 meV for the LCO and CCO, $\sim$32 meV for the SCOC and $\sim$65 meV for the polarimetric spectra. We mapped the magnon dispersion for the three compounds with π polarization along the $(\frac{1}{4}, \frac{1}{4}) \rightarrow (\frac{1}{2}, 0) \rightarrow (0, 0) \rightarrow (\frac{1}{4}, \frac{1}{4})$ path in reciprocal space.

Figure 1 shows the low energy-loss portion of selected spectra (see SM Fig. S2 for the complete set of data [39]).

Each spectrum has been decomposed by phenomenological multipeak fitting into an elastic line at zero energy loss, a phonon contribution and its overtone, a Fano line shape (comprising a leading single-magnon peak and a multimagnon tail), and an additional multimagnon peak, in order of increasing energy loss, as shown in panels (d)–(f) of Fig. 1. The elastic and the multimagnon peaks were modeled using Gaussian functions, while for the phonon peaks we employed a Lorentzian shape convoluted with the experimental resolution. For the additional multimagnon contribution, the choice of line shape is not crucial since the spectrum is very broad energywise. For the single-magnon peak and its tail, we found that the Fano asymmetric function gives the best results in the fitting procedure, and its implications will be discussed below. We emphasize that the peak is not resolution limited for $q > 0.35$ r.l.u. along the [1,0] direction and that a Fano line shape gives much better results across the whole Brillouin zone, especially on the low-energy side of the peak, as compared to a more conventional damped oscillator function [6,44]. The spectra close to $\mathbf{q} = (0, 0)$ are not shown because the elastic component is too intense there and hinders the determination of the loss features. All three compounds show the same asymmetric line shape of the main peak, indicating that this is a common feature of 2D spin-$\frac{1}{2}$ lattices and of cuprates.

The extracted single-magnon peak positions are shown in Figs. 1(a)–1(c) and compared to the INS results taken from literature when available [2,21]. The LCO dispersion is almost superimposed to the INS data over the whole Brillouin zone in agreement with previous literature [3,24,36]. In SCOC, the agreement is very good everywhere except close to the X point. However, the better resolution of our RIXS data with respect to those of Ref. [45], previously used in Ref. [21] for the comparison, allows us to better model the line shape and to reduced the energy difference to $\sim$15 meV. The small
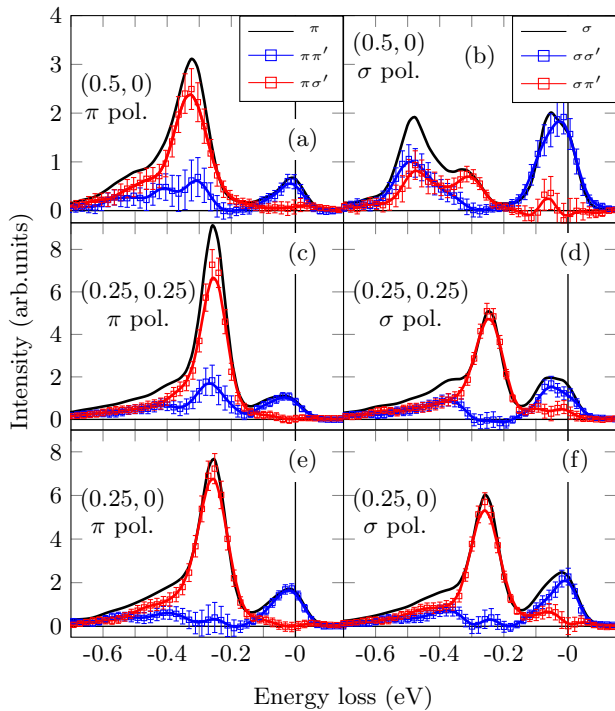
FIG. 2. Polarimetric spectra for SCOC at different **q**. The red and blue solid lines are the result of a three-points-adjacent averaging of the experimental data points (squares). π' and σ' indicate the scattered polarizations.

difference at $(1/2, 0)$ is mainly due to the inadequacy of a single peak to reproduce the actual spectral shape, whose determination is more challenging for INS than RIXS in this region of the momentum space where the scattering intensity is particularly low. Indeed, the X point is characterized by a series of very interesting anomalies (weakening and broadening of the leading magnon peak, emergence of high energy tail) both in theoretical studies [46,47] and in physical realizations of spin-$1/2$ square-lattice antiferromagnetic systems irrespective of the actual exchange energy scale [2,48,49]. We can thus conclude that no significant discrepancy between INS and RIXS single-magnon dispersion remains if the data are measured with adequate energy resolution and statistical quality and are analyzed with the proper line shape.

The richness of the RIXS spectra invites one to go beyond the traditional analysis made on INS data and to better exploit the complexity of the RIXS cross sections. In that spirit, we acquired RIXS spectra of SCOC with analysis of the scattered light polarization at three different **q** values (Fig. 2). Measurement methods, analysis and spectral assignments were made as in Refs. [33,34]. Figure 2(a) confirms that the main peak used to draw the single-magnon dispersion of Fig. 1 has crossed polarization character $\pi\sigma'$ (the prime indicates the scattered x-rays' polarization). The rotation of the photon polarization after the scattering process, which implies a transfer of angular momentum, is needed for an odd number of magnons to be excited, i.e., for $\Delta S = 1$ spin flip process. Conversely the parallel polarization scattering channels must correspond to $\Delta S = 0$ spin conserving excitations, i.e., to an even number of magnons simultaneously excited [50]. With

this in mind, the polarimetric data appear immediately of nontrivial complexity: They disprove the simplistic assignment of the high energy tail to two magnons only and they reveal that parallel polarization spectra are different when π or σ incident polarization is used. The latter is particularly evident by comparing the blue curves of Fig. 2 in panels of the same row, and is very striking at the X point. It is often assumed that, in $\sigma\pi'$ or $\pi\sigma'$ polarization ($\Delta S = 1$ excitations), the scattering involves a single on-site spin-flip operator $\hat{S}_{\mathbf{r}}^{\pm}$, leading to a RIXS spectrum proportional to the transverse magnetic structure factor $S^{\perp}(\mathbf{q}, \omega)$, *irrespective of the relative orientation between electric field and lattice*. From theoretical studies the latter is known to consist of a single-magnon peak and a continuum of odd number of magnons developing above it [18,46,51,52], with the latter having maximum relative spectral weight (40%) at $(1/2, 0)$ [46,47] and around 21% weight on average in the whole Brillouin zone [18]. The crossed polarization line shapes at $(1/4, 1/4)$ and $(1/4, 0)$ [red in Figs. 2(c)–2(f) are consistent with these predictions. Furthermore, the $\pi\sigma'$ polarization at $(1/2, 0)$ shows relatively more weight in the continuum as expected from the theory.

Conversely, the $\sigma\pi'$ polarization at $(1/2, 0)$ does not fit this scenario. Indeed, one might expect $\sigma\pi'$ and $\pi\sigma'$ (red lines) to be proportional to each other and, eventually, to $S^{\perp}((1/2, 0), \omega)$, which is clearly not the case. This implies that the scattering operator in RIXS, in addition to the standard on-site spin-flip process $\hat{S}^{\pm}(\mathbf{r})$ includes nonlocal contributions that can be sensitive to the electric field (i.e., photon polarization) orientation. A possible explanation is a generalization of the three spin operator proposed in Ref. [57], $\hat{S}_{\mathbf{r}}^{\pm}\hat{\mathbf{S}}_{\mathbf{r}} \cdot \hat{\mathbf{S}}_{\mathbf{r}+\delta}$ with a matrix element depending on the projection of the electric field on the bond direction δ. Interference between these two channels allows one to rationalize the need for a Fano line shape for the fitting, and the different spectral shapes between RIXS and INS and between the $\pi\sigma'$ and $\sigma\pi'$ configurations. Multimagnon scattering in RIXS was discussed before [52] as part of the standard $S^{\perp}(\mathbf{q}, \omega)$. Here we propose that the weight of these excitations can be modulated by the photon polarization (see SM [39]).

We now turn to the $\Delta S = 0$ excitations, which can be probed in RIXS as well as Raman and infrared (IR) spectroscopy. In all these cases the scattering operator involves two spin operators $B_{\mathbf{r}}^{\delta} \equiv \hat{\mathbf{S}}_{\mathbf{r}} \cdot \hat{\mathbf{S}}_{\mathbf{r}+\delta}$, and can access excitations with an even number of magnons. In RIXS the scattering operator is usually derived assuming that the main effect of the intermediate $2p^5 3d^{10}$ state is to transiently eliminate one magnetic site. This local approximation [35,57] yields a polarization independent line shape of the even order multimagnon spectrum. However, also in this case, we find that the line shape at the X point is strongly dependent on the polarization (blue lines in Fig. 2), which again calls for nonlocal effects of the core hole. Here the polarization effects can be incorporated already at the leading two-spin operator channel, which facilitates an explicit computation of the spectral shape. Versions of such polarization dependent operators have already been proposed for RIXS [54,58]. We adopt the following form: $A^{nl}(\mathbf{q}) = f(\mathbf{q}) \sum_{\mu} (\hat{\mathbf{e}}^i \cdot \delta)(\delta \cdot \hat{\mathbf{e}}^o) B^{\delta}(\mathbf{q})$. Here $\hat{\mathbf{e}}^{i,o}$ are the polarization vectors of the incoming and outgoing photons and $B^{\delta}(\mathbf{q})$ is the Fourier transform of $B_{\mathbf{r}}^{\delta}$ with $f(\mathbf{q})$ a polarization independent form factor. The resulting line shape is closely
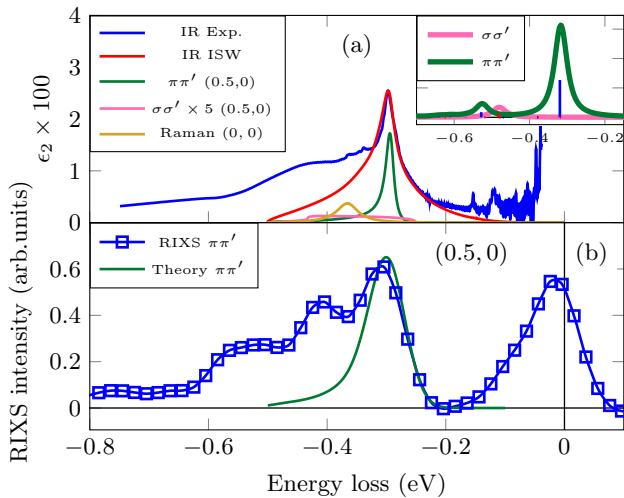
FIG. 3. (a) Blue shows the IR line shape from Ref. [53] plotted as imaginary part of the dielectric function (assuming a dielectric constant $\epsilon_1 = 5$ and a phonon frequency shift of 0.61 meV). The other curves are the interacting spin-wave theory with $J = 0.108$ eV; see Refs. [14–16,54] for details. (b) The $\pi\pi'$ experimental RIXS line shape and the theoretical two-magnon theory with the same energy position used to fit the IR spectra and an experimental Gaussian broadening FWHM = 65 meV. The inset shows the multimagnon response using exact diagonalization in the Heisenberg model in a 32 site cluster as implemented in Refs. [55,56].

related to the theory of phonon-assisted multimagnon excitation, where the same associated spectral function appears but momentum integrated with a different form factor [14–16].

Figure 3(a) shows the IR experiment [53,59] together with an interacting spin-wave theory (ISWT) computation restricted to two magnons [14,15]. This explains the leading peak in terms of the momentum-integrated two-magnon response but misses substantial weight in higher order sidebands, which was thus assigned to four-magnon and higher multimagnon processes [14–16,53,59]. We also show the two-magnon spectral function at specific reciprocal space points, corresponding to the RIXS (green and pink) or Raman (brown) line shape. Upon momentum integration, the IR line shape is dominated by a two-magnon resonance dubbed *the bimagnon*, which corresponds to the proposed RIXS line shape in the $\pi\pi'$ channel at the X point. Indeed, the theoretical bimagnon line shape, whose energy is assigned by the IR experiment, explains fairly well the leading observed RIXS peak [panel (b)]. It may appear surprising that the bimagnon has nearly the same energy as the single magnon [Fig. 2(a)]. This is explained by the attractive magnon-magnon interaction and by the fact that the bimagnon has contributions from low-energy magnons whose individual momentum is away from the zone boundary. Strikingly, it is clear from Fig. 3 that both RIXS and IR leave a similar fraction of spectral weight in higher multimagnon processes, further supporting a common explanation.

In Fig. 3(a) we show also the $\sigma\sigma'$ RIXS two-magnon ISWT prediction, which gives a broad and very weak peak (pink,

multiplied by 5 to make the curves visible) in agreement with the absence of the ≈ 0.3 eV bimagnon peak in the experimental $\sigma\sigma'$ spectrum shown in blue in Fig. 2(b). The structure at ≈ 0.5 eV can be thus assigned to four-magnon and higher multimagnon processes. Indeed, the inset in Fig. 3 shows that the dramatic difference between the two polarization combinations ($\sigma\sigma'$ and $\pi\pi'$) is qualitatively reproduced if instead of restricting to two magnons we perform an exact computation in a small cluster. This treatment, however, underestimates the relative weight of high-energy sidebands. The same problem arises for the IR line shape and was explained as due to finite size effects and a substantial four-ring exchange term in the Hamiltonian [16], which was omitted here for simplicity.

The energy of the bimagnon at $(1/2, 0)$ is constrained by the IR experiments but the dispersion is not. The energy of the bimagnon at $(1/4, 1/4)$ implies a smaller dispersion than in the interacting spin-wave theory computations (SM Fig. S4) which may also be due to extra terms in the Hamiltonian and calls for further theoretical analysis.

Taking full advantage of the additional information contained in the RIXS line shape (both in parallel and crossed polarization channels) requires computations which include nonlocal effects in the scattering cross section and resonant effects in the matrix elements and selection rules, which we hope our work will stimulate. In the future, the present findings can be extended to other magnetic systems and doped cuprate compounds. In IR experiments a remarkably different situation was found for spin-1 2D antiferromagnetic square lattice, where four-magnon and higher order processes remain negligibly weak [15] and the two-magnon theory suffices to reproduce the experimental line shape [60]. We can understand this drastic difference by noting that these computations are based on a $1/S$ expansion, which might pose convergence problems for $S < 1$. Our results are further evidence that $S = 1/2$ systems belong to a different class and are characterized by proximity to more exotic ground states [61], as also proposed earlier by analyzing optical [62] and INS studies [2,48,49].

[1] R. Coldea, S. M. Hayden, G. Aeppli, T. G. Perring, C. D. Frost, T. E. Mason, S.-W. Cheong, and Z. Fisk, Spin Waves and Electronic Interactions in La$_2$CuO$_4$, Phys. Rev. Lett. **86**, 5377 (2001).

[2] N. S. Headings, S. M. Hayden, R. Coldea, and T. G. Perring, Anomalous High-Energy Spin Excitations in the High-T_c Superconductor-Parent Antiferromagnet La$_2$CuO$_4$, Phys. Rev. Lett. **105**, 247001 (2010).

[3] L. Braicovich, J. van den Brink, V. Bisogni, M. M. Sala, L. J. P. Ament, N. B. Brookes, G. M. De Luca, M. Salluzzo, T. Schmitt, V. N. Strocov, and G. Ghiringhelli, Magnetic Excitations and Phase Separation in the Underdoped La$_{2-x}$Sr$_x$CuO$_4$ Superconductor Measured by Resonant Inelastic X-Ray Scattering, Phys. Rev. Lett. **104**, 077002 (2010).

[4] M. P. M. Dean, G. Dellea, R. S. Springell, F. Yakhou-Harris, K. Kummer, N. B. Brookes, X. Liu, Y.-J. Sun, J. Strle, T. Schmitt, L. Braicovich, G. Ghiringhelli, I. Bozovic, and J. P. Hill, Persistence of magnetic excitations in La$_{2-x}$Sr$_x$CuO$_4$ from the undoped insulator to the heavily overdoped non-superconducting metal, Nat. Mater. **12**, 1019 (2013).

[5] M. Minola, G. Dellea, H. Gretarsson, Y. Y. Peng, Y. Lu, J. Porras, T. Loew, F. Yakhou, N. B. Brookes, Y. B. Huang, J. Pelliciari, T. Schmitt, G. Ghiringhelli, B. Keimer, L. Braicovich, and M. Le Tacon, Collective Nature of Spin Excitations in Superconducting Cuprates Probed by Resonant Inelastic X-Ray Scattering, Phys. Rev. Lett. **114**, 217003 (2015).

[6] Y. Y. Peng, E. W. Huang, R. Fumagalli, M. Minola, Y. Wang, X. Sun, Y. Ding, K. Kummer, X. J. Zhou, N. B. Brookes, B. Moritz, L. Braicovich, T. P. Devereaux, and G. Ghiringhelli, Dispersion, damping, and intensity of spin excitations in the monolayer (Bi,Pb)$_2$(Sr,La)$_2$CuO$_{6+\delta}$ cuprate superconductor family, Phys. Rev. B **98**, 144507 (2018).

[7] D. J. Scalapino, A common thread: The pairing interaction for unconventional superconductors, Rev. Mod. Phys. **84**, 1383 (2012).

[8] I. De P.R. Moreira, D. Muñoz, F. Illas, C. De Graaf, and M. A. Garcia-Bach, A relationship between electronic structure effective parameters and T_c in monolayered cuprate superconductors, Chem. Phys. Lett. **345**, 183 (2001).

[9] R. Ofer, G. Bazalitsky, A. Kanigel, A. Keren, A. Auerbach, J. S. Lord, and A. Amato, Magnetic analog of the isotope effect in cuprates, Phys. Rev. B **74**, 220508 (2006).

[10] Y. Y. Peng, G. Dellea, M. Minola, M. Conni, A. Amorese, D. Di Castro, G. M. De Luca, K. Kummer, M. Salluzzo, X. Sun, X. J. Zhou, G. Balestrino, M. Le Tacon, B. Keimer, L. Braicovich, N. B. Brookes, and G. Ghiringhelli, Influence of apical oxygen on the extent of in-plane exchange interaction in cuprate superconductors, Nat. Phys. **13**, 1201 (2017).

[11] O. Ivashko, M. Horio, W. Wan, N. B. Christensen, D. E. McNally, E. Paris, Y. Tseng, N. E. Shaik, H. M. Rønnow, H. I. Wei, C. Adamo, C. Lichtensteiger, M. Gibert, M. R. Beasley, K. M. Shen, J. M. Tomczak, T. Schmitt, and J. Chang, Strain-engineering Mott-insulating La$_2$CuO$_4$, Nat. Commun. **10**, 786 (2019).

[12] A. Grzelak, H. Su, X. Yang, D. Kurzydłowski, J. Lorenzana, and W. Grochala, Epitaxial engineering of flat silver fluoride cuprate analogs, Phys. Rev. Materials **4**, 084405 (2020).

[13] R. R. P. Singh, P. A. Fleury, K. B. Lyons, and P. E. Sulewski, Quantitative Determination of Quantum Fluctuations in the Spin-Planar Antiferromagnet, Phys. Rev. Lett. **62**, 2736 (1989).

[14] J. Lorenzana and G. A. Sawatzky, Phonon Assisted Multimagnon Optical Absorption and Long Lived Two-Magnon States in Undoped Lamellar Copper Oxides, Phys. Rev. Lett. **74**, 1867 (1995).

[15] J. Lorenzana and G. A. Sawatzky, Theory of phonon-assisted multimagnon optical absorption and bimagnon states in quantum antiferromagnets, Phys. Rev. B **52**, 9576 (1995).

[16] J. Lorenzana, J. Eroles, and S. Sorella, Does the Heisenberg Model Describe the Multimagnon Spin Dynamics in Antiferromagnetic CuO Layers? Phys. Rev. Lett. **83**, 5122 (1999).

[17] E. Pavarini, I. Dasgupta, T. Saha-Dasgupta, O. Jepsen, and O. K. Andersen, Band-Structure Trend in Hole-Doped Cuprates and Correlation with $T_{c\,max}$, Phys. Rev. Lett. **87**, 047003 (2001).

[18] J. Lorenzana, G. Seibold, and R. Coldea, Sum rules and missing spectral weight in magnetic neutron scattering in the cuprates, Phys. Rev. B **72**, 224511 (2005).

[19] B. Dalla Piazza, M. Mourigal, M. Guarise, H. Berger, T. Schmitt, K. J. Zhou, M. Grioni, and H. M. Rønnow, Unified one-band Hubbard model for magnetic and electronic spectra of the parent compounds of cuprate superconductors, Phys. Rev. B **85**, 100508(R) (2012).

[20] Y. Wang, E.W. Huang, B. Moritz, and T.P. Devereaux, Magnon Splitting Induced by Charge Transfer in the Three-Orbital Hubbard Model, Phys. Rev. Lett. **120**, 246401 (2018).

[21] K. W. Plumb, A. T. Savici, G. E. Granroth, F. C. Chou, and Young-June Kim, High-energy continuum of magnetic excitations in the two-dimensional quantum antiferromagnet Sr$_2$CuO$_2$Cl$_2$, Phys. Rev. B **89**, 180410(R) (2014).

[22] L. J. P. Ament, M. van Veenendaal, T. P. Devereaux, J. P. Hill, and J. van den Brink, Resonant inelastic x-ray scattering studies of elementary excitations, Rev. Mod. Phys. **83**, 705 (2011).

[23] M. Le Tacon, G. Ghiringhelli, J. Chaloupka, M. M. Sala, V. Hinkov, M. W. Haverkort, M. Minola, M. Bakr, K. J. Zhou, S. Blanco-Canosa, C. Monney, Y. T. Song, G. L. Sun, C. T. Lin, G. M. De Luca, M. Salluzzo, G. Khaliullin, T. Schmitt, L. Braicovich, and B. Keimer, Intense paramagnon excitations in a large family of high-temperature superconductors, Nat. Phys. **7**, 725 (2011).

[24] M. P. M. Dean, R. S. Springell, C. Monney, K. J. Zhou, J. Pereiro, I. Bozovic, B. Dalla Piazza, H. M. Rønnow, E. Morenzoni, J. van den Brink, T. Schmitt, and J. P. Hill, Spin excitations in a single La$_2$CuO$_4$ layer, Nat. Mater. **11**, 850 (2012).

[25] J. Kim, D. Casa, M. H. Upton, T. Gog, Y.-J. Kim, J. F. Mitchell, M. van Veenendaal, M. Daghofer, J. van den Brink, G. Khaliullin, and B. J. Kim, Magnetic Excitation Spectra of Sr$_2$IrO$_4$ Probed by Resonant Inelastic X-Ray Scattering: Establishing Links to Cuprate Superconductors, Phys. Rev. Lett. **108**, 177003 (2012).

[26] D. Betto, Y. Y. Peng, S. B. Porter, G. Berti, A. Calloni, G. Ghiringhelli, and N. B. Brookes, Three-dimensional dispersion of spin waves measured in NiO by resonant inelastic x-ray scattering, Phys. Rev. B **96**, 020409(R) (2017).

[27] G. Fabbris, D. Meyers, J. Okamoto, J. Pelliciari, A. S. Disa, Y. Huang, Z.-Y. Chen, W. B. Wu, C. T. Chen, S. Ismail-Beigi, C. H. Ahn, F. J. Walker, D. J. Huang, T. Schmitt, and M. P. M. Dean, Orbital Engineering in Nickelate Heterostructures Driven by Anisotropic Oxygen Hybridization Rather than Orbital Energy Levels, Phys. Rev. Lett. **117**, 147401 (2016).

[28] Y. Lu, D. Betto, K. Fürsich, H. Suzuki, H.-H. Kim, G. Cristiani, G. Logvenov, N. B. Brookes, E. Benckiser, M. W. Haverkort, G. Khaliullin, M. Le Tacon, M. Minola, and B. Keimer, Site-Selective Probe of Magnetic Excitations in Rare-Earth Nickelates Using Resonant Inelastic X-Ray Scattering, Phys. Rev. X **8**, 031014 (2018).

[29] H. Gretarsson, H. Suzuki, H. Kim, K. Ueda, M. Krautloher, B. J. Kim, H. Yavaş, G. Khaliullin, and B. Keimer, Observation of spin-orbit excitations and Hund's multiplets in Ca_2RuO_4, Phys. Rev. B **100**, 045123 (2019).

[30] G. L. Squires, *Introduction to the Theory of Thermal Neutron Scattering*, 3rd ed. (Cambridge University Press, Cambridge, 2012).

[31] C. Jia, K. Wohlfeld, Y. Wang, B. Moritz, and T. P. Devereaux, Using RIXS to Uncover Elementary Charge and Spin Excitations, Phys. Rev. X **6**, 021020 (2016).

[32] See Supplemental Material [39] for a pedagogic discussion of magnetic scattering in RIXS and neutrons and the distinction between spin-conserving ($\Delta S = 0$) and non spin-conserving ($\Delta S = 1$) scattering processes.

[33] L. Braicovich, M. Minola, G. Dellea, M. Le Tacon, M. Moretti Sala, C. Morawe, J.-Ch. Peffen, R. Supruangnet, F. Yakhou, G. Ghiringhelli, and N. B. Brookes, The simultaneous measurement of energy and linear polarization of the scattered radiation in resonant inelastic soft x-ray scattering, Rev. Sci. Instrum. **85**, 115104 (2014).

[34] R. Fumagalli, L. Braicovich, M. Minola, Y. Y. Peng, K. Kummer, D. Betto, M. Rossi, E. Lefrançois, C. Morawe, M. Salluzzo, H. Suzuki, F. Yakhou, M. Le Tacon, B. Keimer, N. B. Brookes, M. M. Sala, and G. Ghiringhelli, Polarization-resolved Cu L_3-edge resonant inelastic x-ray scattering of orbital and spin excitations in $NdBa_2Cu_3O_{7-\delta}$, Phys. Rev. B **99**, 134517 (2019).

[35] L. Braicovich, L. J. P. P. Ament, V. Bisogni, F. Forte, C. Aruta, G. Balestrino, N. B. Brookes, G. M. De Luca, P. G. Medaglia, F. M. Granozio, M. Radovic, M. Salluzzo, J. van den Brink, and G. Ghiringhelli, Dispersion of Magnetic Excitations in the Cuprate La_2CuO_4 and $CaCuO_2$ Compounds Measured Using Resonant X-Ray Scattering, Phys. Rev. Lett. **102**, 167401 (2009).

[36] H. C. Robarts, M. Barthélemy, K. Kummer, M. García-Fernández, J. Li, A. Nag, A. C. Walters, K. J. Zhou, and S. M. Hayden, Anisotropic damping and wave vector dependent susceptibility of the spin fluctuations in $La_{2-x}Sr_xCuO_4$ studied by resonant inelastic x-ray scattering, Phys. Rev. B **100**, 214510 (2019).

[37] Throughout this work we disregard the out-of-plane momentum and use reciprocal lattice units (r.l.u.) ($2\pi/a$, $2\pi/b$) where $a = b$ are the in-plane lattice parameters of the CuO_2 planes.

[38] N. B. Brookes, F. Yakhou-Harris, K. Kummer, A. Fondacaro, J. C. Cezar, D. Betto, E. Velez-Fort, A. Amorese, G. Ghiringhelli, L. Braicovich, R. Barrett, G. Berruyer, F. Cianciosi, L. Eybert, P. Marion, P. van der Linden, and L. Zhang, The beamline ID32 at the ESRF for soft x-ray high energy resolution resonant inelastic x-ray scattering and polarisation dependent x-ray absorption spectroscopy, Nucl. Instrum. Methods Phys. Res., Sect. A **903**, 175 (2018).

[39] See Supplemental Material at http://link.aps.org/supplemental/10.1103/PhysRevB.103.L140409 for sample details, additional

[40] D. Di Castro, C. Cantoni, F. Ridolfi, C. Aruta, A. Tebano, N. Yang, and G. Balestrino, High-T_c Superconductivity at the Interface between the $CaCuO_2$ and $SrTiO_3$ Insulating Oxides, Phys. Rev. Lett. **115**, 147001 (2015).

[41] S. W. Lovesey, *Theory of Neutron Scattering form Condensed Matter* (Clarendon, Oxford, 1984).

[42] L. J. P. Ament, G. Ghiringhelli, M. M. Sala, L. Braicovich, and J. van den Brink, Theoretical Demonstration of How the Dispersion of Magnetic Excitations in Cuprate Compounds Can Be Determined Using Resonant Inelastic X-Ray Scattering, Phys. Rev. Lett. **103**, 117003 (2009).

[43] M. Cardona, F. Cerdeira, and T. A. Fjeldly, Sign of the Raman tensor of diamond and zinc-blende-type semiconductors, Phys. Rev. B **10**, 3433 (1974).

[44] J. Lamsal and W. Montfrooij, Extracting paramagnon excitations from resonant inelastic x-ray scattering experiments, Phys. Rev. B **93**, 214513 (2016).

[45] M. Guarise, B. Dalla Piazza, M. Moretti Sala, G. Ghiringhelli, L. Braicovich, H. Berger, J. N. Hancock, D. van der Marel, T. Schmitt, V. N. Strocov, L. J. P. Ament, J. van den Brink, P.-H. Lin, P. Xu, H. M. Rønnow, and M. Grioni, Measurement of Magnetic Excitations in the Two-Dimensional Antiferromagnetic $Sr_2CuO_2Cl_2$ Insulator using Resonant X-Ray Scattering: Evidence for Extended Interactions, Phys. Rev. Lett. **105**, 157006 (2010).

[46] A. W. Sandvik and R. R. P. Singh, High-Energy Magnon Dispersion and Multimagnon Continuum in the Two-Dimensional Heisenberg Antiferromagnet, Phys. Rev. Lett. **86**, 528 (2001).

[47] H. Shao, Y. Qi Qin, S. Capponi, S. Chesi, Z. Y. Meng, and A. W. Sandvik, Nearly Deconfined Spinon Excitations in the Square-Lattice Spin-1/2 Heisenberg Antiferromagnet, Phys. Rev. X **7**, 041072 (2017).

[48] N. B. Christensen, H. M. Rønnow, D. F. McMorrow, A. Harrison, T. G. Perring, M. Enderle, R. Coldea, L. P. Regnault, and G. Aeppli, Quantum dynamics and entanglement of spins on a square lattice, Proc. Natl. Acad. Sci. USA **104**, 15264 (2007).

[49] N. Tsyrulin, T. Pardini, R. R. P. Singh, F. Xiao, P. Link, A. Schneidewind, A. Hiess, C. P. Landee, M. M. Turnbull, and M. Kenzelmann, Quantum Effects in a Weakly Frustrated $s = 1/2$ Two-Dimensional Heisenberg Antiferromagnet in an Applied Magnetic Field, Phys. Rev. Lett. **102**, 197201 (2009).

[50] Two-magnon excitations can also contribute in crossed polarization as in Raman but our exact diagonalization calculations show that their energies lie at higher energies.

[51] J.-i. Igarashi and T. Nagao, 1/S-expansion study of spin waves in a two-dimensional Heisenberg antiferromagnet, Phys. Rev. B **72**, 014403 (2005).

[52] J.-i. Igarashi and T. Nagao, Magnetic excitations in L-edge resonant inelastic x-ray scattering from cuprate compounds, Phys. Rev. B **85**, 064421 (2012).

[53] J. D. Perkins, J. M. Graybeal, M. A. Kastner, R. J. Birgeneau, J. P. Falck, and M. Greven, Mid-Infrared Optical Absorption in Undoped Lamellar Copper Oxides, Phys. Rev. Lett. **71**, 1621 (1993).

[54] A. Donkov and A. V. Chubukov, Momentum-dependent light scattering in a two-dimensional Heisenberg antiferromagnet:

data and a pedagogic discussion on magnetic scattering in RIXS and INS, which includes Refs. [40–43].

Analysis of x-ray scattering data, Phys. Rev. B **75**, 024417 (2007).

[55] M. Kawamura, K. Yoshimi, T. Misawa, Y. Yamaji, S. Todo, and N. Kawashima, Quantum lattice model solver HΦ, Comput. Phys. Commun. **217**, 180 (2017).

[56] T. Hoshi, M. Kawamura, K. Yoshimi, Y. Motoyama, T. Misawa, Y. Yamaji, S. Todo, N. Kawashima, and T. Sogabe, $K\omega$–Open-source library for the shifted Krylov subspace method of the form $(z_k I - H)x = b$, Comput. Phys. Commun. **258**, 107536 (2021).

[57] L. J. P. Ament and J. van den Brink, Strong three-magnon scattering in cuprates by resonant x-rays, arXiv:1002.3773.

[58] F. H. Vernay, M. J. P. Gingras, and T. P. Devereaux, Momentum-dependent light scattering in insulating cuprates, Phys. Rev. B **75**, 020403(R) (2007).

[59] J. D. Perkins, R. J. Birgeneau, J. M. Graybeal, M. A. Kastner, and D. S. Kleinberg, Midinfrared optical excitations in undoped lamellar copper oxides, Phys. Rev. B **58**, 9390 (1998).

[60] M. A. Kastner, R. J. Birgeneau, G. Shirane, and Y. Endoh, Magnetic, transport, and optical properties of monolayer copper oxides, Rev. Mod. Phys. **70**, 897 (1998).

[61] P. W. Anderson, P. A. Lee, M. Randeria, T. M. Rice, N. Trivedi, and F. C. Zhang, The physics behind high-temperature superconducting cuprates: The 'plain vanilla' version of RVB, J. Phys.: Condens. Matter **16**, R755 (2004).

[62] C. M. Ho, V. N. Muthukumar, M. Ogata, and P. W. Anderson, Nature of Spin Excitations in Two-Dimensional Mott Insulators: Undoped Cuprates and Other Materials, Phys. Rev. Lett. **86**, 1626 (2001).